Duty cycle modulation - fuzzy logic technique to track the maximum power point of a solar-wind hybrid Source

Clément Kengnou Donfack[1], *Charles Hubert* Kom[1, 2]*, and *Félix* Paune[1]

[1] Laboratory of Computer Science Engineering and Automation, Higher Normal School of Technical Education of Douala, University of Douala, Po Box 2701 Douala, Cameroon
[2] Laboratory of Energy, Materials, Modelling and Methods, National Higher Polytechnic School of Douala, University of Douala, Po Box 2701 Douala, Cameroon

Abstract. In this article, we propose a strategy for finding the maximum power point (MPP) of a hybrid plant (solar and wind), in order to maximize the power extracted from this production plant. This strategy exploits the perturbation and observation method, based on fuzzy logic coupled with the Duty Cycle Modulator (DCM). The main objective of this study is to extract the maximum power from this hybrid power plant, while ensuring the precision and speed of convergence towards this point of maximum power. This method, tested under the Matlab / Simulink environment for a 160 kW hybrid power plant, gave results that we compared to those obtained with the Fuzzy - PWM (Pulse Width Modulator) strategy. It emerges that the Fuzzy-DCM strategy gives better precision (around 2.6 times) and a speed (around 2 times) of convergence compared to the Fuzzy-PWM strategy.

1 Introduction

Since the Earth Conference in Rio de Janeiro, the world has returned to renewable energies to meet its energy demand, in particular wind energy, solar energy, etc. However, their randomness forces the researchers to develop the algorithms to extract the maximum power from these energy sources in order to make the system more cost effective. Indeed, the production of photovoltaic and wind solar energy is impacted by atmospheric conditions, and the operating point of the assembly depends on these conditions and the characteristics of the connected load [1]. For specific load data and atmospheric conditions, there is a single optimal operating point, called the maximum power point (MPP)[2]. Thus, when the source and the load are directly connected to each other, the operating point of the assembly is rarely optimal. To solve this problem, a static converter is used between the source and the load to operate the assembly at the maximum power point. This problem of finding the optimal power is still the subject of several researches until today. Thus, several methods are used in the literature to solve this problem that we can group them into two namely: indirect methods and direct methods [3].
The indirect methods are based on the knowledge of the nonlinear characteristic of the generator, the maximum power point is estimated from the power curve of the generator. These methods are limited by the lack of precision of these characteristic curves (ageing) and the permanent need to measure the sunshine and the ambient temperature for the photovoltaic panels, and the measurement of the wind speed for the wind turbine, then to consult the power curves in order to have the corresponding optimum operating point [4]. However, for the direct methods, the maximum power point is obtained from the measurement of the instantaneous power of the generator. Direct methods do not need to know the power curve of the generator, nor the insolation, nor the temperature, nor the wind speed [5]. The determination of the optimum operating point is independent of climatic conditions. One of the most widely used of these methods is the so-called "disturbance observation". This is justified by its simple structure and the fact that it requires fewer measured parameters. For solar panels, the principle of MPPT consists in varying the power according to the output voltage of the solar panel so that the P-V torque remains at the optimum operating point [6]. And for the wind turbine, the principle of MPPT also consists of varying the power according to the speed of rotation so that the torque P-Ω remains at the point of optimal power [4]. Thus, for a hybrid power plant, each production subsystem has its own MPPT, because they do not act on the same quantities, to find the maximum power point [6]. However, by using the permanent magnet synchronous generator as the aerogenerator of the wind turbine, it is possible for us to use the same MPPT to extract wind and solar energy. Indeed, for a PMG, the wind turbine MPPT is based on the variation of the power of the wind turbine as a function of its rotation speed and according to the power-rotation

*Corresponding author: charleshubert.kom@gmail.com

speed curves, the point of maximum power is reached when the derivative of the power with respect to the speed of rotation is zero ($\frac{dP}{d\Omega} = 0$). And we can rewrite this equation by introducing the derivative of the voltage ($\frac{dP}{d\Omega} = \frac{dP}{dV}\frac{dV}{d\Omega}$). And for a PMG, the generator output voltage is proportional to the rotational speed. Thus, the derivative of the voltage with respect to the rotational speed is always greater than zero ($\frac{dV}{d\Omega} > 0$), and when the maximum power point is reached, only the derivative of the power with respect to the voltage is equal to zero ($\frac{dP}{dV} = 0$). Thus, it can be deduced that the search for the maximum power point of a wind turbine using the PMG, uses the same electrical quantities (power and voltage) to search for the PPM. We can therefore exploit the same MPPT to extract the maximum power from solar and wind generation (MPPT-HYBRID). Since the basic electrical quantities used to determine the maximum power point are voltage and power, the perturbation and observation algorithm is best suited for this purpose [7]. Although having fewer parameters to measure, this algorithm causes permanent oscillations around the MPP. And in addition, if the pulse width modulator is used to drive the DC-DC converter, it will cause convergence speed problem. To solve these problems of oscillation and precision, we will use a fuzzy-DCM controller well adapted to this type of problem because of its fast convergence and its robustness [8]-[9]. For the rest of this article, we will, in section 2, model each component of our system, in particular the solar panels, the wind turbine, the DC-DC converter and its control. And in section 3, the virtual simulations will be made followed by the interpretations of the results.

2 Methodology and research tools

Our structure is basically composed of solar panels, wind turbine, AC/DC rectifier, chopper, load and MPPT Fuzzy-DCM control chain. The following figure 1 shows the diagram of our structure.

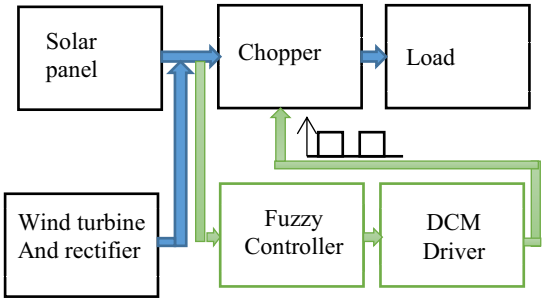

Fig. 1. Bloc diagram of the system.

2.1 Modeling of the photovoltaic panel

The modeling of the solar panel consists in writing the equations linking the current and the tension supplied by the PV according to the solar irradiation and the temperature. The diagram in figure 2 below represents a photovoltaic cell.

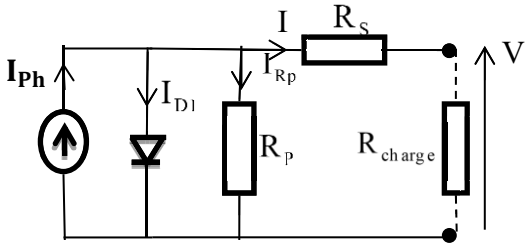

Fig. 2. Diagram of the photovoltaic cell[7].

The current equation I is given by the following relationship[7]:

$$I = I_{ph} - I_0\left(e^{\frac{qV_{D1}}{AKT}} - 1\right) - \frac{(V + R_S I)}{R_p} \quad (1)$$

Where: I_{ph}, I_{D1}, I_{RP}, I, A, T, K, q and I_0 Represent respectively, the photo current from the illuminance, the current in the diode, the current in the parallel resistor and the current in the load, idealistic factor of the cell, temperature of the environment, Boltzmann constant ($138*10^{-23}$ J/K), the electron charge and the reverse saturation current of the diode.

By taking into account the parallel and series connection of the cells in order to form a module, equation (1) can be rewritten as follows [3]:

$$I = N_P I_{ph} - I_0\left(e^{\frac{q\left(\frac{V}{N_S} + \frac{R_S I}{N_P}\right)}{AKT}} - 1\right) - \left(\frac{\frac{N_P V}{N_S} + R_S I}{R_P}\right) \quad (2)$$

Where: Np and Ns Represent respectively, parallel cell number and serial cell number of the module.

And the equation describing the current I_{ph} can be written as follows [7]:

$$I_{Ph} = (I_{CC} + K_i(T - 298.15))\frac{G}{1000} \quad (3)$$

Where: I_{CC}, K_{CC} and G represent respectively the short-circuit current of the cell, the short-circuit temperature coefficient and solar irradiation.

The combination of equations (1), (2) and (3) allows us to plot the power-voltage (P-V) characteristic of the following figure 3:

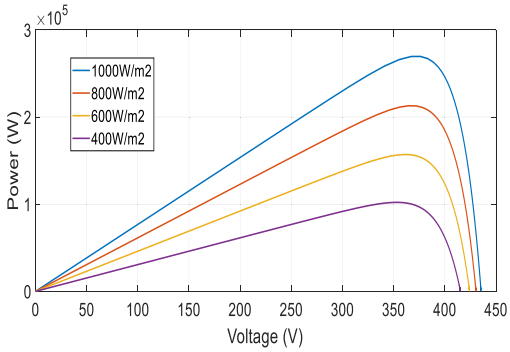

Fig. 3. Power-voltage characteristic of PV [7].

We see in Figure 3 that the increase in solar irradiation leads to an increase in the power produced by the PV and vice versa.

2.2 Modeling of wind power and AC/DC rectifier.

This Modeling consists in giving the voltage and the torque of the PMG according to the speed of the wind in a first time, and in a second time, to give the voltage at the output of the rectifier according to the voltage at the output of the PMG. The following figure 4 shows the diagram of this set.

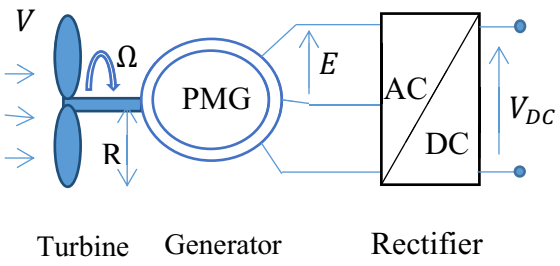

Fig. 4. Diagram of wind power generation.

2.2.1 Medialization of the turbine

Depending on the wind speed (V), the air density (ρ) and the section of the active surface (S) of the wing, the power of the air mass is expressed by [4]:

$$P_V = \frac{1}{2}.\rho.S.V^3 \quad (4)$$

This power cannot be fully captured by the blades of the turbine, so the aerodynamic power is lower than that of the wind, the two powers are linked by the following expression [4]:

$$P = P_v C_p(\lambda,\beta) = \frac{1}{2} C_p(\lambda,\beta).\rho.S.V^3 \quad (5)$$

Where: $\lambda = \frac{R\Omega}{V}$ and $\Omega = 2\pi N$

$C_p(\lambda,\beta)$, λ, Ω, β and N respectively the power coefficient (which is a function of the specific speed (λ) has a maximum of 16/27 called the Betz limit), the specific speed which represents the ratio between the linear speed of the tip of a blade and the wind speed, the angular mechanical speed of the wind turbine rotor (rad/s), the angle of inclination of the blades and the mechanical speed of the wind turbine rotor (tr/s).

This coefficient $C_p(\lambda,\beta)$ can be modeled by the following equation[4]:

$$C_p(\lambda,\beta) = 0.5176\left(\frac{116}{\lambda_1} - 0.4\beta - 5\right)e^{\frac{-21}{\lambda_1}} + 0.006\lambda \quad (6)$$

Where: $\lambda_1 = \frac{1}{\lambda + 0.08\beta} - \frac{0.035}{\beta^3 + 1}$

Fig.5 represents the characteristics (Cp-λ) for different values of the angle of inclination of the blades β. The maximum value of Cp-pmax is obtained for β = 0° and λ = 10.99 and figure 6 represents the characteristics (P-N), for different values of the wind speed.

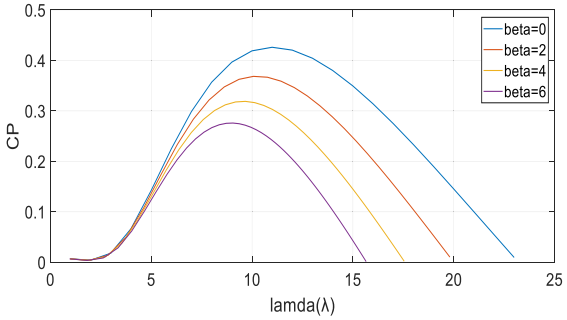

Fig.5. Characteristics *Cp-λ*

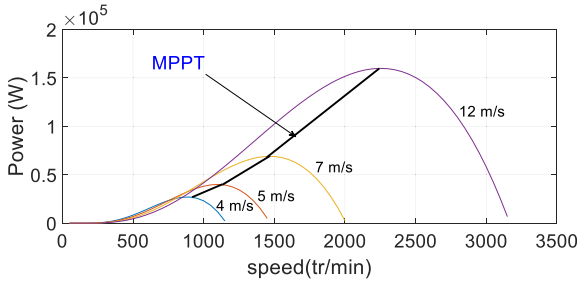

Fig.6. Characteristics P-N

We see in Figure 6 that the power and the speed of rotation of the turbine increase with the wind speed. And for each speed, there is a maximum power point of the turbine that we can extract. Thus, for all the rotational speeds, an MPPT algorithm can be developed, making it possible to extract, at any time, the maximum power of the turbine.

2.2.2 Modeling of the generator (PMG)

The PMG generator transforms the mechanical energy of the turbine into electrical energy. Its modeling consists in determining the expression of the tension and the torque according to the speed of rotation of the turbine (therefore the speed of the wind).
For a generator to be able to produce a voltage, it must be excited (for PMG, the excitation is permanent and constant), and its rotor must be in motion (in rotation). Tension and torque expressions can be given by the following equations[10]:

$$V = K_e N \quad (7)$$

$$Tem = K_t I \quad (8)$$

Where: K_t, K_e, I and V respectively, the torque coefficient, the voltage coefficient, the stator current and the voltage induced across the PMG. Figures 7, 8 and 9 below show us the curves of voltage at the output of PMG as a function of rotational speed (V-N) for $K_e = 0.138$, for power as a function of voltage (P-V) and of torque as a function of current (T-I) in the load for $K_t = 1.1145$

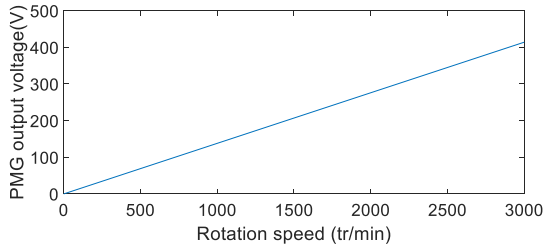

Fig. 7. Characteristics V-N

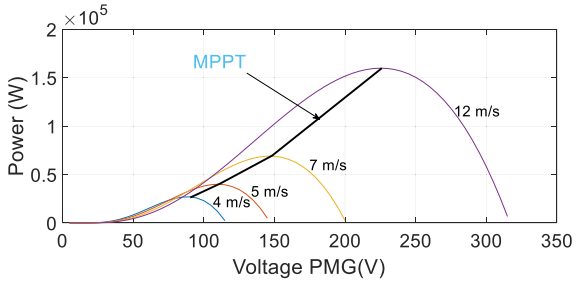

Fig. 8. Characteristics P-V

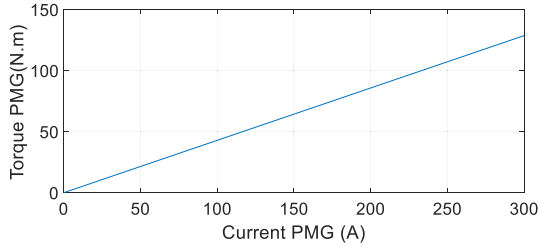

Fig.9. Characteristics T-I

These two figures show us that the torque is proportional to the current and the voltage is proportional to the speed of rotation. Thus, we can act on the speed of rotation by acting on the voltage at the terminal of the PMG.

2.2.3 Rectifier modeling

The objective of this modeling consists in determining the output voltage of the converter according to its input voltages (of the PMG). This rectifier is an uncontrolled three-phase bridge.
The voltage and current at the output of this three-phase bridge as a function of the voltages and current of the PMG can be determined by the expressions of the following average values [10]:

$$U_{DC} = \frac{3\sqrt{6}}{\pi} U_{PMG} \quad (9)$$

$$I_{DC} = \frac{\pi}{\sqrt{6}} I_{PMG} \quad (10)$$

Where U_{DC} and I_{DC}, respectively represent the average output voltage and current of the rectifier, and represent the rms values of the fundamental voltage and current of the PMG generator.
We find that voltage (U_{DC}) and current (I_{DC}) depend on voltage (U_{PMG}) and current (I_{PMG}). Thus, the increase in the continuous load (DC) will have an impact on the voltage at the terminals of the PMG, therefore on its speed of rotation (ω). It is thus possible to seek the maximum power point, using only the continuous values of the rectifier (U_{DC} and I_{DC}).

2.3 Chopper modeling.

The chopper is a DC/DC converter whose role is to raise or lower the DC voltage. In this article, its role is to raise the voltage from the solar panels and the wind rectifier, in order to extract the maximum power from them. The diagram in figure 10 below is the electrical model of this chopper.

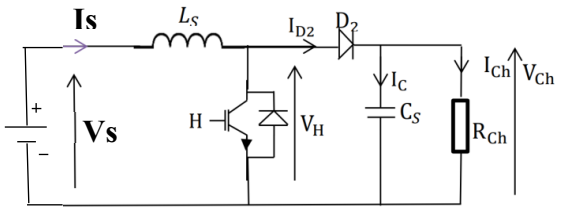

Fig. 10. Boost chopper diagram[7]

The modeling of the boost chopper consists here in determining the expression of the voltage and the current of the load (therefore of the power of the load), according to the input voltage and the duty cycle D. The expression of this the modeling can be represented by the following equations 11 and 12 [7].

$$\begin{cases} V_{ch} = \dfrac{V_s}{1-D} \\ I_{ch} = \dfrac{V_{ch}}{R_{ch}} = \dfrac{V_s}{(1-D).R_{ch}} \end{cases} \quad (11)$$

$$P_{ch} = V_{ch} I_{ch} = \frac{V_{ch}^2}{(1-D)^2.R_{ch}} \quad (12)$$

We see on equation 12, that we can vary the power of the load by acting on the duty cycle D, thus, we can increase the power of the load by increasing the duty cycle and vice versa. This variation of the duty cycle will be carried out by the MPPT-Fuzzy DCM command.

2.4 Modeling of the MPPT-Fuzzy DCM command.

2.4.1 MPPT algorithm

The extraction of the maximum power exploits the method of disturbance and observation in a fuzzy logic therefore the MPPT algorithm is represented in the following figure 11 [7] :

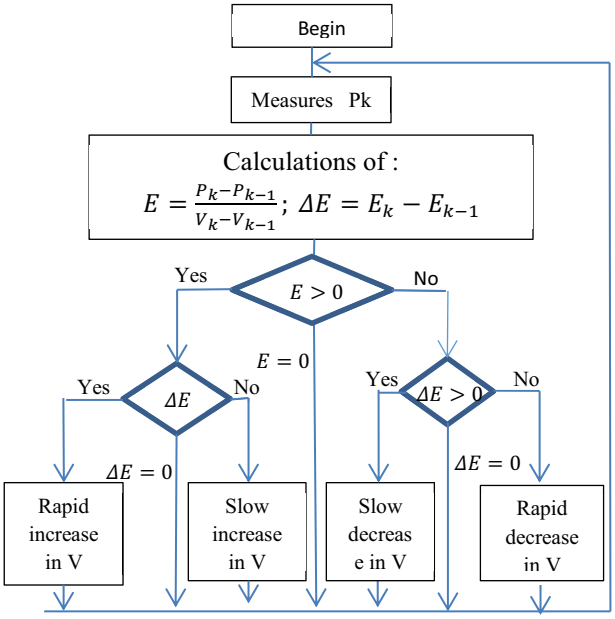

Fig. 11. Algorithm MPPT.

Where:

$$E = \frac{dP}{dV} = \frac{P_k - P_{k-1}}{V_k - V_{k-1}} \quad (13)$$

$$dE = \frac{d^2P}{dV^2} = E_k - E_{k-1} \quad (14)$$

2.4.2 *Fuzzy Controller Modeling.*

Three steps/blocks are sufficient to model the fuzzy controller: fuzzification (the fuzzification block is used to transform the measured input quantities into fuzzy quantities E and dE), inference (Inference Block a rule base, which contains the definition of the terms used in the command and the rules characterizing the target of the command and describing the behavior of the expert) and the defuzzification (Block defuzzification on output, which determines a precise action from the fuzzy descriptions of the output variables). Figure 12 below shows us this controller.

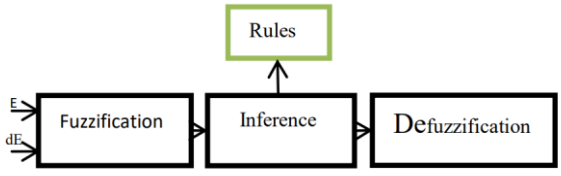

Fig.12. Basic structure of fuzzy logic [7].

We attribute to them the following linguistic variables: Very Negative (TN), Negative (N), Zero (Z), Positive (P) and Very Positive (TP). Their membership functions are shown in figure 13 below.

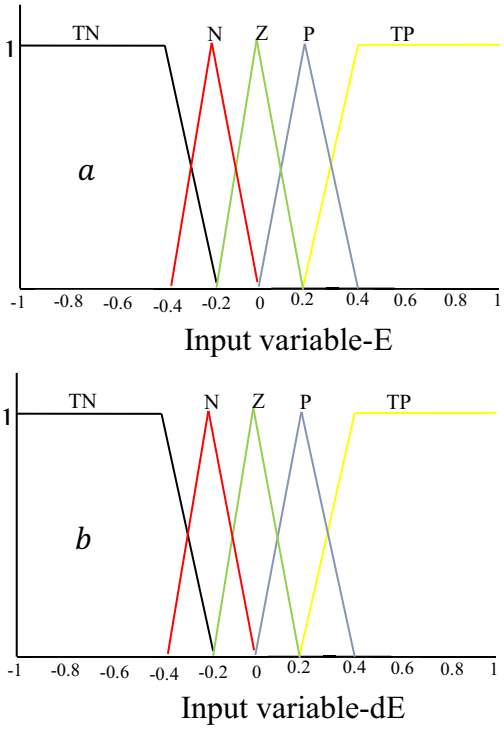

Fig.13. Membership functions of inputs.

2.4.3 *DCM and PWM modulator modeling*

The DCM is a relaxation oscillator whose principle is taken from that of tantalum vase. This modulator is under deep studies since 2005[8]. Today, it is totally master in term of modelling and optimisation of its intrinsic parameters that makes it operate in linear mode. Basically, it based on the use of a negative resistor and it structure presents a double feedback as shown in figure 14-a[7]. The role of the DCM and PWM modulators is to convert the duty cycle from the fuzzy controller into a pulse allowing us to extract the maximum power from the PV and wind power. The modeling thus consists in giving the pulses produced by these modulators according to the input signal. Figure 14-a shows the DCM [8] and Figure 14-b shows the PWM [11].

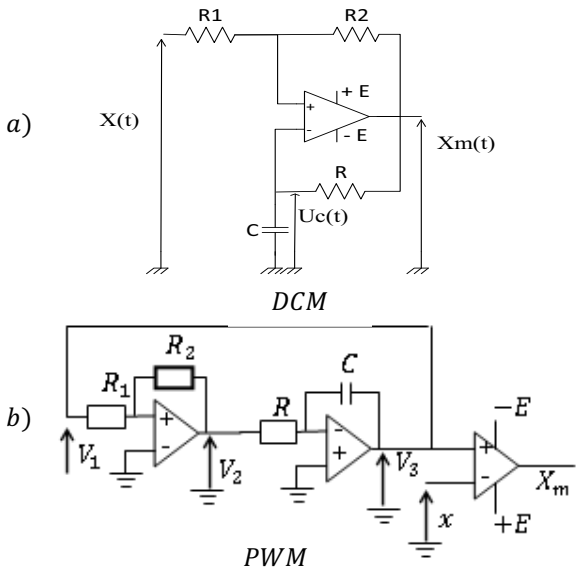

Fig.14. Diagram of the DCM and PWM [8]-[11]

These two modulators are characterized by their duty cycles (Rm) and their operating frequencies (F) [8]. The equations below, give the expressions of the duty cycle and the operating frequency of each modulator.

For PWM_[11]

Oscillation frequency $F(x)_m$

$$T(x)_m = 4R1RC / R2 \quad (15)$$

Duty cycle R_m

$$R_m = \frac{1}{2}[1 - \frac{x}{E}.\frac{R2}{R1}] \quad (16)$$

For DCM_[8]

Oscillation frequency $F(x)_m$

$$T(x,\alpha)_m = \tau \log\left[\frac{(\beta x)^2 - ((1-\alpha)E)^2}{(\beta x)^2 - ((\alpha-1)E)^2}\right] \quad (1)$$

And its duty cycle R_m

$$R_m = \frac{T_{on}(x,\alpha)}{T(x,\alpha)_m} \quad (2)$$

$$R_m = \frac{\log\left[\frac{(1-\alpha)x - ((1+\alpha)E)}{(1-\alpha)x - ((\alpha-1)E)}\right]}{\log\left[\frac{(\beta x)^2 - ((1-\alpha)E)^2}{(\beta x)^2 - ((\alpha-1)E)^2}\right]} \quad (19)$$

The linearization of this cycle ratio gives us [8] :

$$R_m = \frac{\alpha x}{E(1+\alpha)\log(\frac{1+\alpha}{(1-\alpha)})} + \frac{1}{2} \quad (20)$$

We can see that the frequency of the PWM is fixed whatever the value of the input signal and only its duty cycle varies with the input signal x. For the DCM modulator, we find that the duty cycle and frequency vary with the input signal, which allows the DCM modulator to be faster and more accurate than the PWM.

3 Simulation and analysis of results

The simulations are done in MATLAB Simulink R2017b software. The two modulators having the same operating frequency and the same input signal, are compared on the basis of the response time and on the amplitudes of the oscillations around the bridge of maximum power.

3.1 Simulation diagram.

The figure 15 below shows the simulation diagram of our structure. Data: G= [1000, 900], T=30C, V= [11m/s, 9m/s] P=160 kW and F=50 kHz.

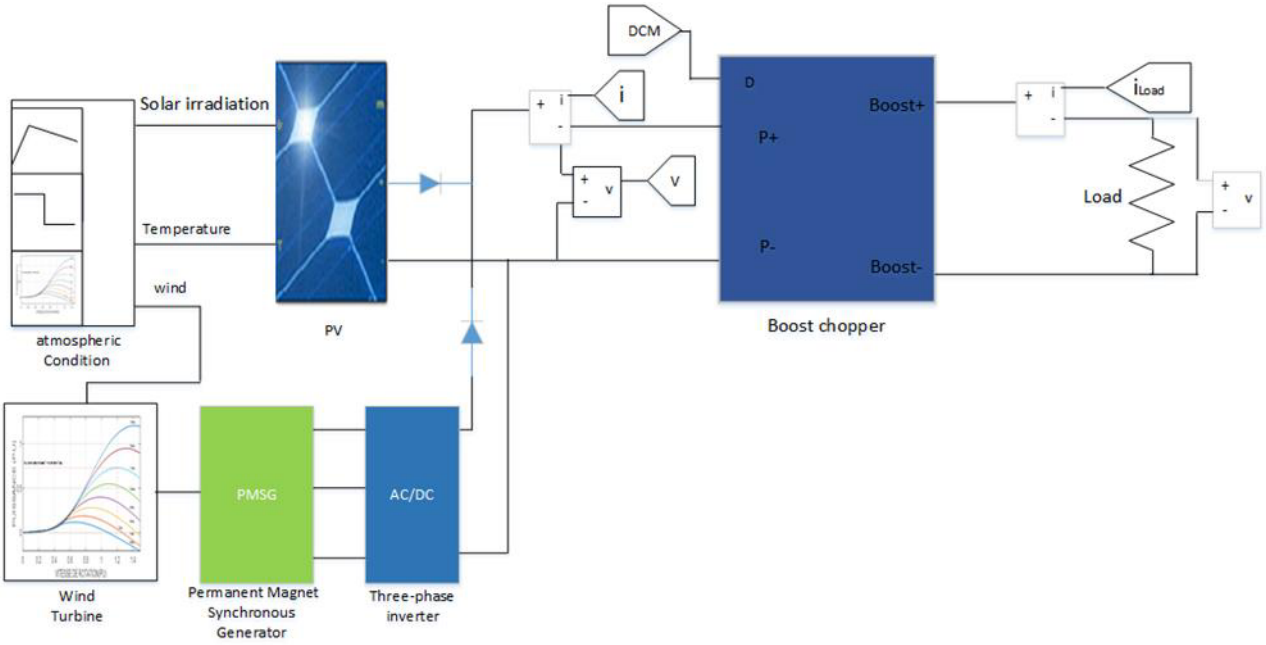

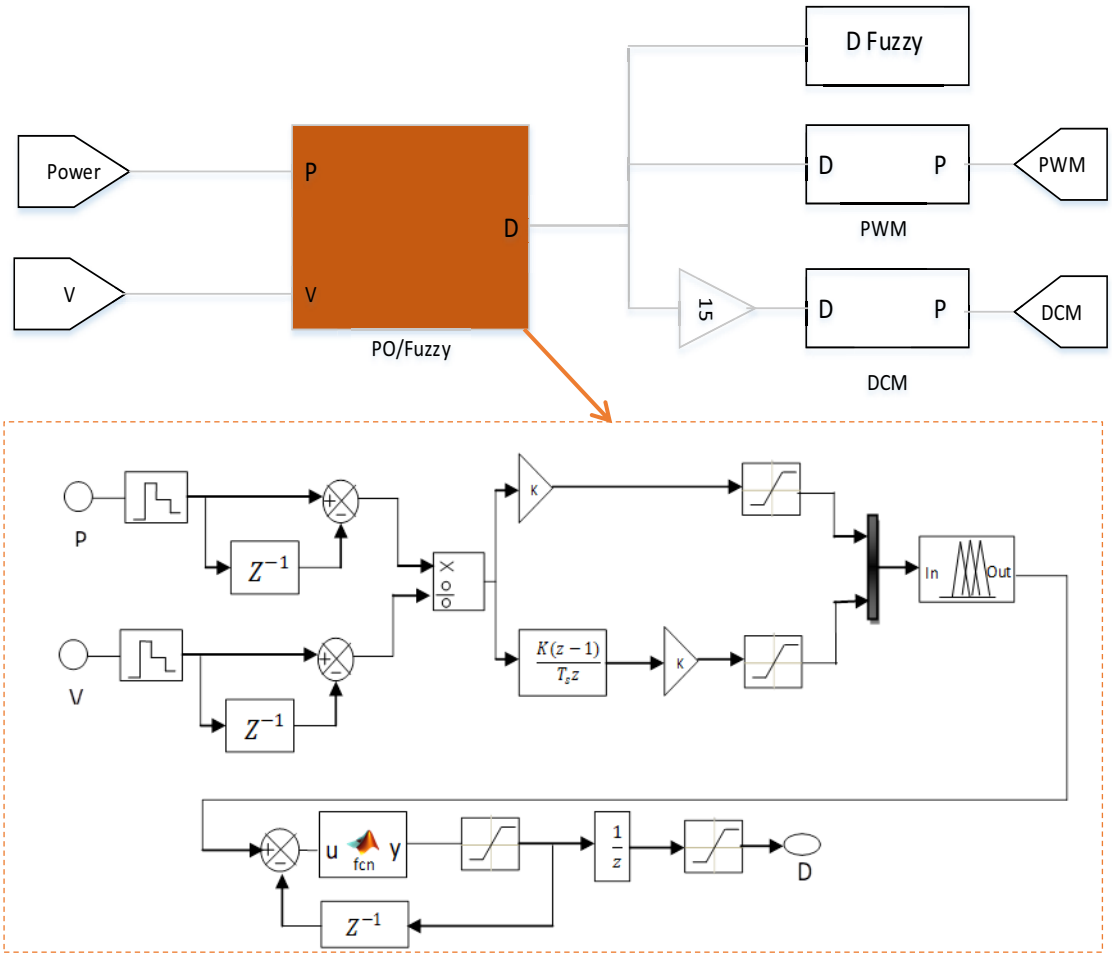

Fig.15. Simulation diagra

3.2 Simulation results.

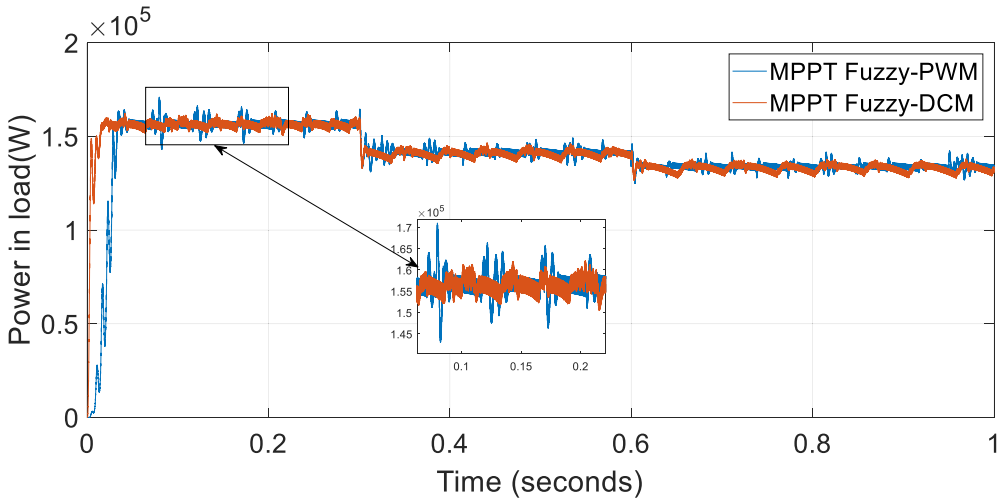

Fig.16. Power in load.

3.3 Analysis of results

3.3.1 Analysis of results for solar irradiation of 1000W/m² and wind speed of 11 m/s

From 0s to 0.3s, the solar radiation is 1000 W/m² and a wind speed of 11m/s. Table 1 below gives us the power variation at the load terminals.

Table 1. Power variation for 1000W/m² and V=11m/s.

	PWM	DCM
Response time(s)	0.033	0.015
Pmax(kW)	170.98	161.97
Pmin(kW)	142.97	151.72
ΔP(kW)	27.93	10.72

We find that the DCM modulator is faster (2 times faster) and causes less (2.60 times less) power oscillation compared to the PWM modulator.

3.3.2 Analysis of the results for solar radiation of 900W/m2 and a wind speed of 11 m/s.

From 0.3s to 0.6s, the solar radiation is 900 W/m2 and a wind speed of 11m/s. Table 2 below gives the power variation at the load terminals.

Table 2. Power variation for 900W/m2 and V=11m/s.

	PWM	DCM
Pmax(kW)	149.03	145.16
Pmin(kW)	134.42	135.04
ΔP(kW)	14.61	10.12

We find that the DCM modulator causes less (1.44 times less) power oscillation compared to the PWM modulator.

3.3.3 Analysis of results for solar irradiation of 900W/m2 and wind speed of 9 m/s

From 0.6s to 0.7s, the solar radiation is 900 W/m² and a wind speed of 9m/s. Table 3 below gives the power variation at the load terminals.

Table 3. Power variation for 900W/m2 and V=9m/s.

	PWM	DCM
Pmax(kW)	141.60	137.35
Pmin(kW)	127.54	127.74
ΔP(kW)	14.06	9.61

We find that the DCM modulator causes less (1.46 times less) power oscillation compared to the PWM modulator.

4 Conclusion

In this article, it was a question of extracting the maximum power from renewable energies, in particular solar and wind, by exploiting the same DC/DC converter controlled by the DCM in order to reduce the oscillations around the MPP and also to improve the speed of convergence towards this point. To do it, we first described the perturbation and observation algorithm widely used today to extract the maximum powers of renewable energies, then the limits of this algorithm were described later. And we proposed a new method to extract the maximum power from a hybrid plant (PV and wind). This method is based on the Perturbation and Observation method and fuzzy logic-DCM (MPPT Fuzzy DCM). This new method is tested on a 160 kW hybrid power plant and the test results show that it is faster (2 times) and more accurate (2.6 times) than the Fuzzy-PWM MPPT. In the future, it would be more interesting to implement this method in a real system, and in addition to seek to improve the results by exploiting other intelligent methods.

References

1. M. N. Ali, K. Mahmoud, M. Lehtonen, et M. M. F. Darwish, « Promising MPPT Methods Combining Metaheuristic, Fuzzy-Logic and ANN Techniques for Grid-Connected Photovoltaic », *Sensors (Basel)*, vol. 21, nº 4, p. 1244, févr. 2021, doi: 10.3390/s21041244.
2. S. M et D. Kumar, « Fuzzy Based MPPT Controller For Solar Photovoltaic Systems », *International Journal of Advanced Research in Science, Communication and Technology*, p. 359-370, mai 2021, doi: 10.48175/IJARSCT-1095.
3. H. Doubabi, I. Salhi, M. Chennani, et N. Essounbouli, « High Performance MPPT based on TS Fuzzy–integral backstepping control for PV system under rapid varying irradiance—Experimental validation », *ISA Transactions*, vol. 118, p. 247-259, déc. 2021, doi: 10.1016/j.isatra.2021.02.004.
4. H. Baccar, Z. Moncef, N. Mensia, et M. Bouaicha, « Maximisation du Rendement d'Un Générateur Eolien à Base d'Une Génératrice Synchrone à Aimant Permanent », Symposium de Génie électrique, oct. 2017, vol. 14, p. 65-72.
5. A. J. H. A. Gizi, « PLC Fuzzy PID Controller of MPPT of Solar Energy Converter », *WSEAS Transactions on Systems and Control*, vol. 16, p. 1-20, 2021, doi: 10.37394/23203.2021.16.1.
6. M. Qasim et V. Velkin, « Maximum Power Point Tracking Techniques for Micro-Grid Hybrid Wind and Solar Energy Systems - a Review », *International Journal on Energy Conversion (IRECON)*, vol. 8, p. 223, nov. 2020, doi: 10.15866/irecon.v8i6.19502.
7. clément K. Donfack, C. H. Kom, et B. M. Lonla, « Duty Cycle Modulation and Fuzzy Controller of a Chopper Extracting the Maximum Power Point of a Solar Panel », *International Journal of Renewable Energy Research (IJRER)*, vol. 12, nº 1, Art. nº 1, mars 2022.
8. S. G. Béatrice et M. Jean, « FPGA-Based Analog-to-Digital Conversion via Optimal Duty-Cycle Modulation », *Electrical and Electronic Engineering*, vol. 8, nº 2, p. 29-36, 2018, doi: 10.5923/j.eee.20180802.01.

*Corresponding author: charleshubert.kom@gmail.com

9. P. O. Etouke, L. N. Nneme, et J. Mbihi, « An Optimal Control Scheme for a Class of Duty-Cycle Modulation Buck Choppers: Analog Design and Virtual Simulation », *Journal of Electrical Engineering, Electronics, Control and Computer Science*, vol. 6, nº 1, p. 13-20, 2020.
10. Minh Huynh Quang, « Optimisation de la production de l'electricite renouvelable pour site isole », Thèse Doctorat, Phd, Universite de Reims Champagne-Ardenne, 2015.
11. G. M. Ngaleu, C. H. Kom, A. T. Yeremou, S. Eke, et A. Nanfak, « Design of New Duty-Cycle Modulator Structures for Industrials Applications, an Alternative to Pulse-Width Modulation », *EJEE*, vol. 23, nº 2, p. 103-111, avr. 2021, doi: 10.18280/ejee.230203.